

Transmission Measurement of Quality Factor in Two-Dimensional Photonic-Crystal Microcavity

Edmond Chow^{*a}, S.Y. Lin^{**b}, S.G. Johnson^c and J.D. Joannopoulos^c

^aAgilent Technologies Lab., ^bSandia National Lab., ^cMassachusetts Institute of Technology

ABSTRACT

A new micro-cavity design is proposed and structures are realized using a 2D photonic-crystal slab. The cavity consists of seven defect holes that encompass a hexagon and is designed to reduce vertical light leakage. From a direct transmission measurement, a Q-value of 816 ± 30 is achieved at $\lambda = 1.55 \mu\text{m}$. This high-Q cavity will enable realistic realization of spontaneous emission modification and on-off optical switches.

Keywords: Photonic crystal, microcavity

1. INTRODUCTION

The realization of high quality (Q) micro-cavity at optical wavelength (λ) has many important technological consequences. According to the Purcell effect [1], spontaneous emission rate can be greatly altered inside a high-Q cavity [2-4]. A high-Q cavity also operates as a bandpass filter for on-off optical switching application [5]. A photonic crystal, a periodically arranged dielectric sub- λ structure, offers a unique optical environment for creating such a cavity. Its ability to confine light strongly will lead to the creation of high-Q cavities at optical λ with a small size ($\sim \lambda^3$). Moreover, its sub- λ feature permits great geometrical flexibility in designing micro-cavities. By using different types and combinations of local defects, cavity resonant frequency and mode symmetry can both be varied [4].

While a three-dimensional (3D) photonic-crystal is most ideal for creating high-Q cavities [6,7], 1D or 2D photonic-crystal is advantageous in their fabrication simplicity [8-13]. Recently, Foresi *et. al.* realized a micro-cavity with $Q=265$ using a four-period ($N=4$) 1D photonic-crystal [14]. For 2D photonic-crystal cavities, there are several reports on the analysis of Q-factors; mostly estimated from top-emitting photoluminescence data [11-13,15]. One exception is the work by Labilloy *et. al.* who use guided luminescence to probe a horizontal cavity and obtain a Q-value of 200 for $N=9$ [10]. A top-scattering geometry was also suggested for add-drop-filter application [16]. Although, top emitting is a result of light leakage in the vertical direction, which limits cavity-Q. A direct transmission measurement of 2D crystal cavities at optical λ is currently lacking, due mainly to difficulties of precise lateral waveguide coupling. In this paper, we report direct measurements of Q-factor of 2D photonic-crystal micro-cavities at $\lambda \sim 1.55 \mu\text{m}$. Using a new cavity design that minimizes vertical leakage, cavity-Q is shown to increase exponentially with N and a $Q=814$ is achieved for $N=4$.

2. CAVITY DESIGN

Our photonic crystal consists of 2D triangular array of holes, etched through a GaAs slab. The 2D hole-array has a lattice constant $a=440\text{nm}$. The hole-diameter is $d=0.6a=264\text{nm}$ and the etched-depth $\sim 0.6\mu\text{m}$. The GaAs slab is 220nm thick ($t=0.5a$) and sandwiched between a $2\mu\text{m}$ thick Al_xO_y layer and a $0.1\mu\text{m}$ SiO_2 layer. Previous measurement has shown that the photonic-crystal has a large TE-like (transverse electric) photonic band gap, from $0.255 < \omega(a/\lambda) < 0.325$ [17]. Within the gap, light is guided inside and near the proximity of GaAs slab through index guiding [17-19]. The field thus decays exponentially in the air and substrate, and vertical radiation losses are only possible when translation symmetry is broken, e.g., by a defect-cavity. Our micro-cavity consists of seven smaller holes, hole-diameter $d'=0.4a=176\text{nm}$, that encompass a hexagon and is called a "super-defect". A SEM image of the 2D hole-array and micro-cavity is shown in Fig.1. A cavity may also be introduced by changing the radius of a single hole, however our calculation predicts that its Q-factor is low. In this case, the radiation Q (Q_r), which describes the rate of decay of the cavity mode into the air, is always under 500 and usually under 250 [20]. The super-defect design, on the other hand, is expected to have a much higher Q_r ($Q_r > 1,000-2,000$) and its resonant frequency near the middle of the TE gap (mid-gap). One drawback of this design is that cavity-size is slightly increased to $\sim 0.1 \mu\text{m}^3$ (or a volume of 1.5 time $(\lambda/n)^3$), cavity-mode slightly de-localized and doubly degenerate. Here, n is refractive index of GaAs.

*edmond_chow@agilent.com; phone 1-650-485-5152; fax 1-650-485-7852; Agilent Technologies, Inc. MS 26M-9B, 3500 Deer Creek Rd., Palo Alto, CA 95124. ** slin@sandia.gov

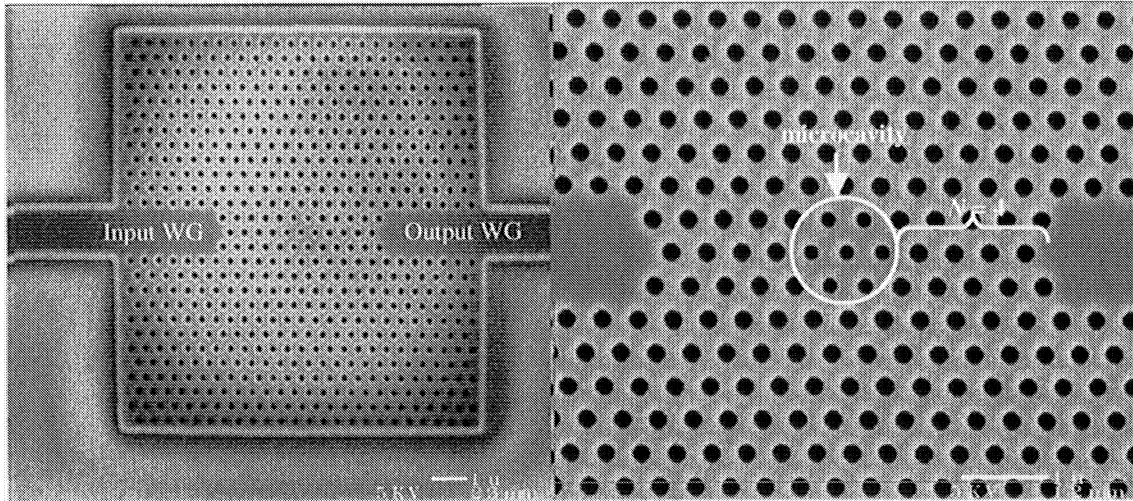


Fig.1, SEM top-view image of a microcavity sample. The microcavity consists of seven smaller holes, with hole diameter $d'=0.4a=176\text{nm}$, that encompass a hexagon. The input and output waveguides are used to facilitate coupling of laser light. The four periods ($N=4$) of a photonic crystal act as a photonic tunnel barrier for confinement of light.

Another loss mechanism is decay of cavity mode into adjacent wave-guides and is described by Q_w . As shown in Fig.1, the cavity is separated from the input and output wave-guides by four periods, $N=4$, of photonic crystal. The photonic crystal acts as a photon tunnel barrier for light to couple from input guide to cavity and then decays back to the output guide. The decaying rate, and therefore Q_w , has an exponential dependence on tunnel barrier thickness, i.e. Na_0 [21]. The total Q_t is given by: $1/(Q_t) = 1/(Q_w) + 1/(Q_r)$. As Q_w can, in principle, be increased by increasing N , Q_r sets the upper limit for Q_t . To realize a high- Q cavity, it is essential to have a cavity design that maximizes Q_r . It is equally important to demonstrate that Q_w depends on N exponentially [22]. For this experiment, three nominally identical cavities with different N s, $N = 2, 3$ and 4 , are fabricated on the same chip.

3. DATA

A high-resolution tunable diode laser with scanning step $=0.02\text{nm}$ is used to obtain the transmission spectrum. The laser beam is linearly polarized and focused into an input wave-guide by a high numerical aperture microscope objective. The output light is split and fed into an InGaAs photo-detector for intensity measurement and an infrared camera for mode profile monitoring. This procedure ensures that only the guiding mode signal is fed into the detector.

Fig.2 (a) shows a TE transmission spectrum (black circles) taken from an $N=2$ super-cavity sample. The data has a vertical offset of 0.1 for clarity. The spectrum shows a transmission peak at $\lambda \sim 1547\text{nm}$, or equivalently $\omega(a/\lambda)=0.2846$, which is at the TE mid-gap. It also contains multiple wavelength oscillations, with a periodicity of $\Delta\lambda \sim 0.55\text{nm}$. This value of $\Delta\lambda$ corresponds to a resonant cavity of length $L \sim 0.6\text{mm}$, which is the distance between the waveguide end-facet and waveguide-crystal interface. The oscillations are thus attributed to end facets Fabry-Perot resonance and not derived from micro-cavity resonance.

The same measurement is repeated for an $N=4$ cavity sample and transmission spectrum (black circles) shown in Fig.2 (c). The data has a vertical offset of 0.08 for clarity. The spectrum shows a better-defined transmission peak as well as short-period oscillations. The oscillations have the same period ($\Delta\lambda \sim 0.55\text{nm}$) as that for the $N=2$ sample, and are due to end-facets Fabry-Perot resonance. Yet, the main transmission peak exhibits several distinct features. First, its peak position shifts slightly to $\lambda \sim 1551\text{nm}$, $\omega(a/\lambda)=0.2836$, but is still near the TE mid-gap. Secondly, its line-width becomes much narrower, its line-shape more symmetrical

and Lorentzian-like. Thirdly, background transmission away from the peak, i.e. $\lambda < 1545$ and $\lambda > 1555$ nm, is near zero. The line-width narrowing, the improvement in line-shape as N is increased and the fact that peak position is within the TE gap, all suggest that the observed transmission peak originates from cavity resonance.

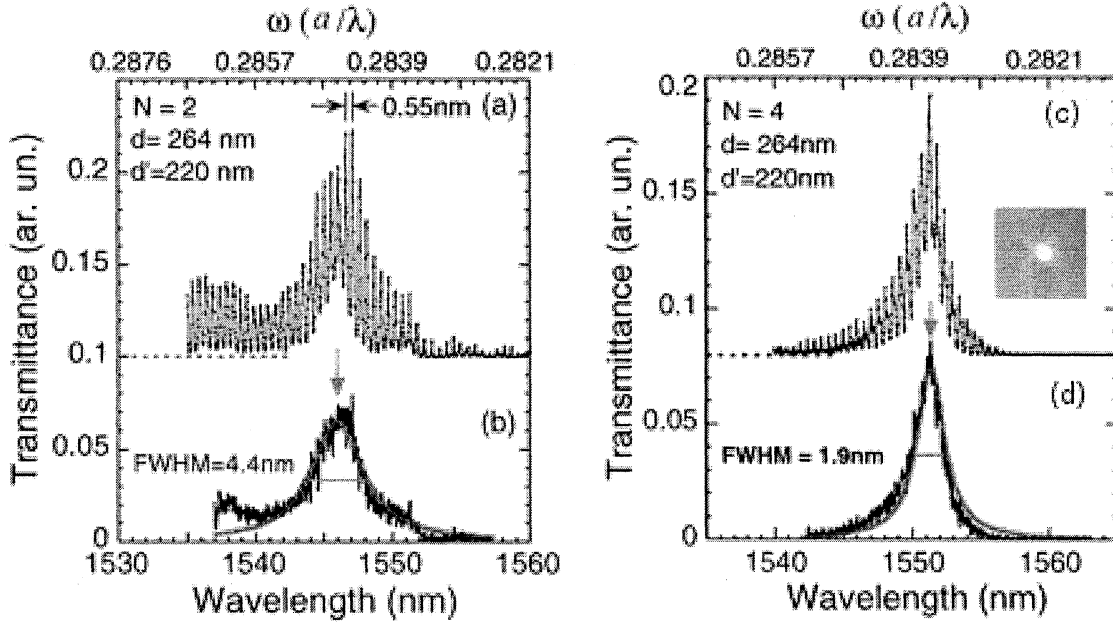


Fig.2 Transmission spectrum for $N=2$ (left) and $N=4$ (right) microcavity sample. (a) and (c) The raw data of spectrum shows a transmission peak at $\lambda \sim 1547$ nm and $\lambda \sim 1551$ nm respectively with short period oscillations $\Delta\lambda \sim 0.55$ nm. (b) and (d) Smoothed data fitted to a Lorentzian (gray curve); the deduced FWHM are 4.4 nm and 1.9 nm for $N=2$ and $N=4$ respectively. Inset in Fig. 2c shows the infrared image of transmitted light has a well-defined Gaussian-like profile.

Further transmission measurements, with a TM (transverse magnetic) polarized light, were carried out for the same samples. As there is no TM gap in this wavelength range, $\lambda = 1510$ - 1590 nm, no transmission peak is observed. Nonetheless, the Fabry-Perot oscillations persist for TM polarization. This measurement further confirms that the observed peak is due to the presence of a TE photonic band gap.

To obtain a more accurate Q-value, we first perform a Fourier transform for the raw data and remove the part of Fourier component due to Fabry-Perot oscillations. We then apply an inverse Fourier transform to obtain the data, which is plotted as circles shown in Fig. 2(b) and 2(d), respectively. The data is then fitted to a Lorentzian function and the red curve represents the fit. The experimental Q-factor is given by $Q_r = \lambda / \Delta\lambda_{FWHM}$, where λ is the peak wavelength and $\Delta\lambda_{FWHM}$ the full-width-at-half-maximum (FWHM). For $N=2$, the experimental ω and Q -values are $\omega = 0.2846$ and $Q_r = 351 \pm 20$, respectively. For $N=4$, $\omega = 0.2837$ and $Q_r = 816 \pm 30$, which is 3 times higher than that for the 1D crystal microcavity of $N=4$ [14]. This is expected as light in a 1D cavity leaks both vertically and laterally to the sides. The measured ω also agrees with the theoretical value of $\omega = 0.2933$ within 4% [23]. For our $N=4$ cavity, a large spontaneous emission enhancement rate, $\eta \sim Q / (\Delta V / \lambda^3) = 514$, can be achieved. Additionally, for a cavity-Q of 816, an index modulation ($\delta n/n$) as small as 1.3×10^{-3} is sufficient for tuning cavity- ω for on-off optical switching application [5].

4. SUMMARY

In Fig.4, we plot cavity Q-factor (solid circles) in a logarithmic scale and cavity- ω (red squares) as a function of number-of-periods ($N=2, 3, 4$). While the observed ω varies by less than 1%, the Q-value increases sharply as N is increased from 2 to 4. The observed Q-factors are then fitted to an exponential function, $Q_f=Q_0 * \exp(\kappa N a)$, with κ as a fitting parameter. The fit is good and the deduced κ is $0.90 \pm 0.05 (\mu\text{m})^{-1}$. Here, κ is a measure of light trapping strength of the two photonic tunnel barriers that bound the cavity mode. A similar exponential dependence has also been reported in microwave range for an ideal 2D photonic crystal [9, 24]. This exponential dependence suggests that the observed increase in Q is due to an increase in photonic crystal mirror reflectivity. It further suggests that Q_f is significantly larger than Q , and a higher Q-value is achievable by increasing N . The small variation in cavity- ω may be due to the uncertainty in defect hole-size.

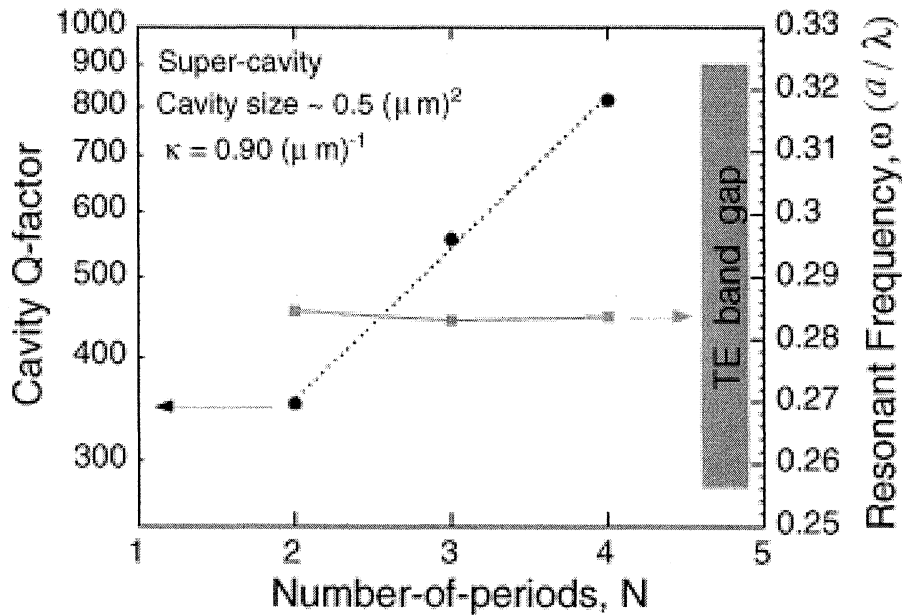


Fig. 4. Summary of resonant frequency (filled squares) and cavity Q-factors (filled circles) as a function of N . The observed resonant frequency (ω) is at the TE midgap and varies less than 1% for all samples. The cavity Q factors are fitted to an exponential function (dashed line), and the deduced slope is $\kappa = 0.9 (\mu\text{m})^{-1}$.

In summary, a new micro-cavity design is proposed and structures realized using a 2D photonic-crystal slab. The cavity Q-factor is measured to be 816 ± 30 for an $N=4$ cavity. Such a high-Q cavity will enable realistic realization of spontaneous emission modification and optical on-off switches.

ACKNOWLEDGEMENTS

The research at Sandia National Laboratories is supported by the U.S. Department of Energy. Sandia is a multiprogram laboratory operated by Sandia Corporation, a Lockheed Martin Company, for the U.S. Department of Energy under contract DE-AC04-94AL 85000.

REFERENCES

- [1] E.M. Purcell, *Phys. Rev.* **69**, 681 (1946).
- [2] S. Haroche and D. Kleppner, *Phys. Today* **42**, 24 (1989).
- [3] H. Yokoyama, *Science* **256**, 66 (1992).
- [4] E. Yablonovitch, *J. Op. Soc. Am. B* **10**, 283 (1993).
- [5] P.R. Villeneuve, D.S. Abrams, S. Fan and J. D. Joannopoulos, *Op. Lett.* **21**, 2017 (1996).
- [6] E. Ozbay, G. Tuttle, M. Sigalas, C.M. Soukoulis, and K.M. Ho, *Phys. Rev B* **51**, 13961 (1998).
- [7] S.Y. Lin, J.G. Fleming, M.M. Sigalas, R. Biswas, and K.M. Ho, *Phys. Rev. B* **59**, 15579 (1999).
- [8] D.R. Smith, R. Dalichaouch, N. Kroll, S. Schultz, S.L. McCall and P.M. Platzman, *J. Op. Soc. Am. B* **10**, 314 (1993).
- [9] S.Y. Lin, V.M. Hietala, S.K. Lyo and A. Zaslavsky, *Appl. Phys. Lett.* **68**, 3233 (1996).
- [10] D. Labilloy, H. Benisty, C. Weisbuch, T.F. Krauss, V. Bardinal and U. Oesterle, *Electronics Lett.* **33**, 1978 (1997).
- [11] P. Potter, C. Seassal, X. Letartre, J.L. Leclercq, P. Viktorovitch, D. Cassagne and C. Jouanin, *J. Lightwave Tech.* **17**, 2058 (1999).
- [12] J.-K. Hwang, H.-Y. Ryu, D.-S. Song, I.-Y. Han, H.-W. Song, H.-K. Park, Y.-H. Lee, *Appl. Phys. Lett.* **76**, 2982 (2000).
- [13] O.J. Painter, A. Husain, A. Scherer, J.D. O'Brien, I. Kim and P.D. Dapkus, *J. Light Wave Tech.* **17**, 2082 (1999). Estimate of the upper bound Q value of 600 has been reported using photoluminescence measurements.
- [14] J.S. Foresi, P.R. Villeneuve, J. Ferrera, E.R. Thoen, G. Steinmeyer, S. Fan, J.D. Joannopoulos, L. C. Kimberling, H. I. Smith and E.P. Ippen, *Nature* **390**, 143 (1997).
- [15] In such a measurement, luminescence transition linewidth must be de-convoluted to allow for a quantitative analysis of cavity linewidth and therefore cavity-Q.
- [16] S. Noda, A. Chutinan, M. Imada, *Nature* **407**, 608 (2000).
- [17] E. Chow, S.Y. Lin, S.G. Johnson, P.R. Villeneuve, J.D. Joannopoulos, J.R. Wendt, G.A. Vawter, W. Zubrzycki, H. Hou and A. Alleman, *Nature* **407**, 983 (2000).
- [18] S. G. Johnson, S. Fan, P.R. Villeneuve, J.D. Joannopoulos, and L.A. Kolodziejski, *Phys. Rev. B* **60**, 5751 (1999).
- [19] P.R. Villeneuve, S. Fan, S. G. Johnson, and J.D. Joannopoulos, *IEE Proc. Optoelec.* **145**, 384 (1998).
- [20] For single-hole defect cavity calculation, the hole-diameter is varied from $d'=0.3-1.0a$. For the super-cavity, hole-diameter is varied from $d'=0.3-0.5a$.
- [22] S.Y. Lin and G. Arjavalingam, *Op. Lett.* **18**, 1666 (1993).

[23] When other losses, such as dielectric loss and TE- to-TM mode conversion loss, become compatible to tunneling loss, this dependence is no longer valid.

[24] For a description of calculation method, refer to *Appl. Phys. Lett.* 78, 3388 (2001).

[25] T. Ueta, K. Ohtaka, N. Kawai and K. Sakoda, *Appl. Phys. Lett.* **84**, 6299 (1998).